C.P. No 115
(15,029)
A.R.C. Technical Report

MINISTRY OF SUPPLY

AERONAUTICAL RESEARCH COUNCIL

CURRENT PAPERS

The Application of the Polygon Method to the Calculation of the Compressible Subsonic Flow round Two-dimensional Profiles

By

F/Lt. L. C. Woods, M.A., D.Phil., A.F.R.Ae.S.,
(R.N.Z.A.F. Scientific Defence Corps,
seconded to the Aerodynamics Division, N.P.L.)

LONDON HER MAJESTY'S STATIONERY OFFICE

1953

Price 7s 6d net

C.P. No.115

The Application of the Polygon Method to the Calculation of the Compressible Subsonic Flow round Two-dimensional Profiles

- By -

F/Lt. L. C. Woods, M.A., D.Phil., A.F.R.Ae.S.,
(R.N.Z.A.F. Scientific Defence Corps,
seconded to the Aerodynamics Division of the N.P.L.)

27th June, 1952

Summary

This paper sets out the method now used by the author of applying the polygon method[1] to the calculation of the compressible subsonic flow round two-dimensional aerofoils. Tables have been constructed which can be used for all aerofoil shapes, putting the polygon method on the same footing numerically as Goldstein's "Approximation III"[2] for incompressible flow. However the polygon method has the advantage over Approximation III that it can be applied in the following cases which are beyond the scope of Goldstein's method:- (a) the "high subsonic" (without shock wave) compressible flow about conventional aerofoils, (b) the low-speed flow about very thick aerofoils, e.g., in reference 3 it is applied to circular cylinders, (c) the flow about symmetric aerofoils between either straight or constant pressure walls[3], (d) flow in asymmetric channels, and (e) more difficult problems of the flow about aerofoils in the presence of one or two constraining walls (to be published). A method of calculating lift and moment coefficients, and their rates of change with incidence (α) is also given in the paper.

As an example the velocity distribution and the rates of change of the lift and moment coefficients with α are calculated for the aerofoil R.A.E.104 at values of M_∞ (Mach number at infinity) of 0, and 0.7, for various values of the incidence, α. The velocity distributions for zero incidence are found to be in fair agreement with the corresponding experimental results. The results at incidence are in satisfactory agreement with the experimental results, not for the same incidence, but for the same lift coefficient. It is found, for example, that at $M_\infty = 0.7$ the theory for $\alpha = 0.8^\circ$ agrees best with experiment for $\alpha = 1.0^\circ$, when the lift coefficients are approximately the same.

Definition of Symbols

(x,y)	$z = x + iy$, $(i = \sqrt{-1})$, the physical plane
(ϕ,ψ)	$w = \phi + i\psi$, the plane of equipotentials (ϕ = constant) and streamlines (ψ = constant) for zero circulation
(q,θ)	velocity vector in polar co-ordinates for zero circulation
α	angle of incidence measured from the zero lift angle

(q_α,θ_α)/

Published with permission of the Director, National Physical Laboratory.

Definition of Symbols (contd.)

(q_α,θ_α)	velocity vector appropriate to angle of incidence α
U	velocity at infinity
L	$\equiv \log(U/q)$
s	distance measured along the aerofoil surface
$2\tau_a, 2\tau_b$	leading and trailing edge angles respectively
θ_s, θ_a	symmetrical and antisymmetrical parts of θ on the aerofoil surface
$1/R$	$= -\left(\dfrac{d\theta}{ds}\right)_{\eta=0}$, the curvature of the aerofoil surface
M	Mach number
β	$\equiv (1 - M^2)^{\frac{1}{2}}$ (subsonic); $\equiv (M^2 - 1)^{\frac{1}{2}}$ (supersonic)
∞	as a suffix to denote values at infinity
ρ, ρ_o	the local and stagnation densities respectively
m	$\equiv (1 - M^2)^{\frac{1}{2}} \rho_o/\rho = \rho_o\beta/\rho$; $m_\infty = \rho_o\beta_\infty/\rho_\infty$
(η, γ)	elliptic co-ordinates defined by $\phi + im_\infty\psi = -2a\cosh(\eta + i\gamma)$, the aerofoil surface is $\eta = 0$, when $\phi = -2a\cos\gamma$
$4a$	the length of the slit representing the aerofoil in the (ϕ,ψ) plane
C_p	pressure coefficient for compressible flow
C_{p_o}	pressure coefficient for incompressible flow
δ	$\equiv (q/U - 1)$.

1. Introduction

This paper sets out some advances in the application of the author's polygon method[1] of calculating the two-dimensional inviscid compressible flow about aerofoils in unbounded streams. The polygon method for incompressible flow is based on an exact integral equation, which can be readily solved by a rapidly convergent iterative process. The corresponding integral equation for compressible flow is derived in reference 1 with the aid of an approximation due to von Kármán[6]. A full discussion on this point appears in section 4 below, where, on the basis of experimental evidence, the author suggests a modification of the Kármán-Tsien law relating C_p and C_{p_o}.

The polygon method can be applied to a variety of two-dimensional fluid motion problems. (See references 3, 4 and 10; a report will be published soon extending the method to flow in doubly-connected regions.) The integral equation on which it is based

(equation/

(equation (13) below) is in fact the conjugate equation to that used in the "exact" method of aerofoil design[4,11]. This means that Tables 2 and 3 of this report, which were originally constructed to facilitate the calculation of the flow about a given aerofoil are equally useful in designing aerofoils to have a given velocity distribution[4].

The principal effect of incidence on the boundary conditions is to shift the front stagnation point along the aerofoil surface, and thus to reverse the flow direction over a small region of the boundary. From this consideration the author has developed a new method of calculating the contribution to the solution due to incidence. This method which is given in the next section, has the advantage over the method given in reference 1 of being applicable to more difficult problems of the flow about aerofoils in the presence of one or two constraining walls.

2. The Basic Equations

On the assumption that

$$n = n_{co}, \qquad \ldots (1)$$

it has been shown, that for zero circulation (see reference 1, §12),

$$r + i\theta = \frac{i}{2\pi} \int_{-\pi}^{\pi} \theta(y^*) \coth \tfrac{1}{2}(iy^* - iy - \eta)\, dy^*,$$

where

$$r \equiv \int_{q=U}^{q} (1 - M^2)^{\frac{1}{2}}\, d\left(\log \frac{U}{q}\right), \qquad \ldots (2)$$

and $\theta(y^*)$ is the value of θ on the aerofoil surface. Since $\theta(y^*) = \theta(2\pi + y^*)$, an integration by parts results in

$$r + i\theta = -\frac{1}{\pi} \int_{y^*=-\pi}^{\pi} \log \sinh \tfrac{1}{2}(iy^* - iy - \eta)\, d\theta(y^*). \qquad \ldots (3)$$

It is a simple matter to deduce the effect of incidence on this equation. The L.E. (front stagnation point for <u>zero incidence</u>) will be assumed to be at $y = 0$, then, since on the aerofoil surface $\phi = -2a \cos y$, the T.E. (rear stagnation point for <u>all incidences</u>) will be at $y = \pi$. The effect of incidence on the stagnation points is to leave the rear stagnation point unchanged in position (Joukowski Condition) and to shift the front stagnation point around the aerofoil surface. Suppose that placing the aerofoil at an incidence α, which decreases $\theta(y^*)$ by an amount α in $-\pi < y^* \leqslant \pi$, moves the front stagnation point from $y = 0$ to $y = -\delta$. Then in the interval $-\delta \leqslant y^* \leqslant 0$ the flow direction on the aerofoil surface will be reversed, i.e., $\theta - \alpha$ will be increased by an amount π in this range. Thus the increment $\Delta\theta$, to $\theta(y^*)$ due to incidence is given by

θ = /

$$\theta = \begin{cases} -\alpha, & -\pi < y \leqslant -\delta \\ \pi - \alpha, & -\delta \leqslant y \leqslant 0 \\ -\alpha, & 0 \leqslant y \leqslant \pi. \end{cases}$$

Substituting this result in equation (3) we find

$$r_\alpha + i\theta_\alpha = r + i\theta - \frac{1}{\pi}\left\{- i\pi\alpha + \pi \log \frac{\sinh \frac{1}{2}(\eta + iy + i\delta)}{\sinh \frac{1}{2}(\eta + iy)}\right\}.$$

Since by definition

$$\phi + im_\infty\psi = -2a \cosh(\eta + iy), \qquad \dots (4)$$

$\eta = \infty$ is at infinity in the physical plane. Thus $\lim_{\eta \to \infty} q = U$, and so from (2), $\lim_{\eta \to \infty} r = 0$. Thus applying $\lim_{\eta \to \infty}$ to the equation for $r_\alpha + i\theta_\alpha$ we obtain $r_{\alpha\infty} = r_\infty = 0$, $\theta_{\alpha\infty} = \theta_\infty + \alpha - \frac{1}{2}\delta$, and since the flow at infinity must be undisturbed by incidence, $\delta = 2\alpha$. Thus the equation for $r_\alpha + i\theta_\alpha$ reads

$$r_\alpha + i\theta_\alpha = r + i\theta + i\alpha - \log \frac{\sinh \frac{1}{2}(\eta + iy + 2i\alpha)}{\sinh \frac{1}{2}(\eta + iy)}. \qquad \dots (5)$$

An alternative proof of equation (5) not based on equation (3) is given in reference 1.

Equation (3) can be expanded in powers of $e^{-\eta}$, then, since from (4),

$$\phi + im_\infty\psi = -a\, e^{\eta + iy}\{1 + O(e^{-2\eta})\},$$

we find

$$r + i\theta = -\frac{1}{\pi}\int_{y^*=-\pi}^{\pi}\left\{\log(-\tfrac{1}{2}) + \frac{\eta + iy}{2}\right\} d\theta(y^*) + \frac{i}{2\pi}\int_{y^*=-\pi}^{\pi} y^*\, d\theta(y^*)$$

$$- \frac{a}{\pi(\phi + im_\infty\psi)}\int_{y^*=-\pi}^{\pi} e^{iy^*}\, d\theta(y^*) + O\left(\frac{1}{\phi + im_\infty\psi}\right)^2.$$

Now/

Now zero circulation implies that $\log \dfrac{q}{U} = O\left(\dfrac{1}{\phi + i m_\infty \psi}\right)^2$ near infinity (c.f. §7.4 in reference 12), and since $\lim_{\eta \to \infty} (r + i\theta) = i\theta_\infty$, it follows from the above expansion of $r + i\theta$ that

$$\int_{y^*=-\pi}^{\pi} \cos y^* \, d\theta(y^*) = \int_{y^*=-\pi}^{\pi} \sin y^* \, d\theta(y^*) = \int_{y^*=-\pi}^{\pi} d\theta(y^*) = 0, \qquad \ldots (6)$$

and

$$\theta_\infty = \frac{1}{2\pi} \int_{y^*=-\pi}^{\pi} y \, d\theta(y^*) . \qquad \ldots (7)$$

Equations (6), which are equivalent to the condition that the aerofoil is a closed contour, are required in the numerical application of equation (3) to a given aerofoil. An alternative method of establishing them is given in reference 4.

Finally, since by definition

$$d\phi = q \, ds \, , \; d\psi = \frac{\rho}{\rho_0} q \, dn \, ,$$

then on the aerofoil surface

$$\frac{sU}{2a} = \frac{1}{2a} \int_{-2a}^{\phi} \frac{U}{q} \, d\phi = \int_0^y \frac{U \sin y}{q} \, dy \, , \qquad \ldots (8)$$

where n is distance measured normal to a streamline, and s is distance measured along a streamline. In equation (8) the origin of s has been taken at the front stagnation point. Equations (1) to (8) are the basic equations of the polygon method.

3. Numerical Solution of the Basic Equations

The aerofoil surface is $\psi = 0$, when from (4), $\eta = 0$, and

$$\phi = -2a \cos y \, . \qquad \ldots (9)$$

In the limit as $\eta \to 0$, equations (3) and (5) yield

$$r = -\frac{1}{\pi} \int_{y^*=-\pi}^{\pi} \log \sin \tfrac{1}{2}(y^* - y) \, d\theta(y^*), \qquad \ldots (10)$$

and/

and

$$r_a = r - \log \frac{\sin \frac{1}{2}(y + 2a)}{\sin \frac{1}{2}y} . \qquad \ldots(11)$$

When θ is continuous

$$d\theta = \frac{d\theta}{ds}\frac{ds}{d\phi}\frac{d\phi}{dy^*} dy^* ,$$

i.e., from equation (9),

$$d\theta = -\left(\frac{2a \sin y^*}{R\, q}\right) dy^* \qquad \ldots(12)$$

where $R \left(= -\dfrac{ds}{d\theta}\right)$ is the radius of curvature; otherwise suppose there are simple discontinuities τ_j at γ_j in θ; then (10) can be expanded:-

$$r = \frac{1}{\pi}\left(\frac{2a}{Uc}\right)\int_{-\pi}^{\pi}\left(\frac{cU}{Rq}\right) \sin y^* \log \sin \tfrac{1}{2}(y^* - y) dy^*$$

$$- \frac{1}{\pi}\sum_j \tau_j \log \sin \tfrac{1}{2}(\gamma_j - y) , \qquad \ldots(13)$$

in which c is the aerofoil chord. For simplicity only the L.E. and T.E. discontinuities ($2\tau_a$ at $y^* = 0$, and $2\tau_b$ at $y^* = \pi$, see Figure 1) will be considered in this report.

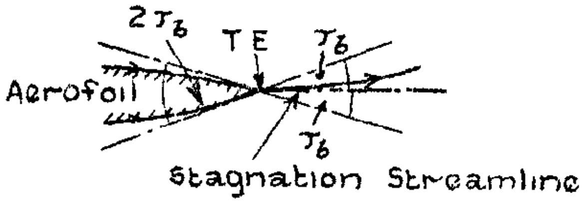

FIG 1.

If

$$C \equiv \tfrac{1}{2}\left(\frac{2a}{Uc}\right)\left\{\frac{cU}{Rq}(y^*) - \frac{cU}{Rq}(-y^*)\right\} \sin y^* ,$$

$$D \equiv \tfrac{1}{2}\left(\frac{2a}{Uc}\right)\left\{\frac{cU}{Rq}(y^*) + \frac{cU}{Rq}(-y^*)\right\} \sin y^* ,$$

equation/

equation (13) can be written

$$r(\pm y) = \frac{1}{\pi}\int_0^{\pi}\left\{C \log \sin \tfrac{1}{2}(y^* - y)\sin \tfrac{1}{2}(y^* + y) \pm D \log \frac{\sin \frac{1}{2}(y^* - y)}{\sin \frac{1}{2}(y^* + y)}\right\} dy^*$$

$$- \frac{2\tau_a}{\pi} \log \sin \tfrac{1}{2}y - \frac{2\tau_b}{\pi} \log \cos \tfrac{1}{2}y.$$

Now the range $(0,\pi)$ is subdivided into $(y_2, y_3, \ldots y_i \ldots y_{n-1}, y_n)$, where $y_2 = 0$, $y_n = \pi$, such that it can be assumed, with negligible error, that C and D are constant and equal to their mid-range values in each interval; thus if matrices A, B, C and D are defined by

$$A_{ik} = -\frac{1}{\pi}\int_{y_i}^{y_{i+1}} \log \sin \tfrac{1}{2}(y^* - y_k)/\sin \tfrac{1}{2}(y^* + y_k)\,dy^*, \quad i, k = 2, 3 \ldots n-1,$$

$$B_{ik} \begin{cases} = -\dfrac{2}{\pi} \log \sin y_k & i = 1,\ k = 2, 3 \ldots n-1 \\[2ex] = -\dfrac{1}{\pi}\displaystyle\int_{y_i}^{y_{i+1}} \log \sin \tfrac{1}{2}(y^* - y_k)\sin \tfrac{1}{2}(y^* + y_k)\,dy^*, & i, k = 2, 3 \ldots n-1, \\[2ex] = -\dfrac{2}{\pi} \log \cos y_k & i = n,\ k = 2, 3 \ldots n-1 \end{cases}$$

$$C_i \begin{cases} = \tfrac{1}{2}\left(\dfrac{2a}{Uc}\right)\left\{\dfrac{cU}{Rq}(y_{i+\frac{1}{2}}) - \dfrac{cU}{Rq}(-\,y_{i+\frac{1}{2}})\right\} \sin y_{i+\frac{1}{2}}, & i = 2, 3 \ldots n-1 \\[2ex] = -\,\tau_a & i = 1, \\[1ex] = -\,\tau_b & i = n \end{cases}$$

$$D_i = \tfrac{1}{2}\left(\frac{2a}{Uc}\right)\left\{\frac{cU}{Rq}(y_{i+\frac{1}{2}}) + \frac{cU}{Rq}(-\,y_{i+\frac{1}{2}})\right\} \sin y_{i+\frac{1}{2}}, \quad i = 2, 3 \ldots n-1,$$

where

$$y_{i+\frac{1}{2}} = \tfrac{1}{2}(y_i + y_{i+1}),$$

then/

then the equation for r can be written

$$r(\pm y_k) = -\sum_{i=1}^{n} C_i B_{ik} \mp \sum_{i=2}^{n-1} D_i A_{ik}, \quad k = 2, 3 \ldots n-1. \qquad \ldots(14)$$

$\int_0^x \log \sin \frac{1}{2}t \, dt$ has been tabulated[5], and so there is no difficulty in calculating A_{ik} and B_{ik} for a given subdivision of $(0,\pi)$. For a symmetrical aerofoil $R(y^*)$ is an antisymmetric function, and so

$$D_i = 0, \; C_i = \left(\frac{2a}{Uc}\right)\left(\frac{cU}{Rq}\right) \sin y_{i+\frac{1}{2}}, \; i = 2, 3 \ldots n-1. \qquad \ldots(15)$$

A small modification needs to be made to the above scheme. For a rounded-nose aerofoil, $D(y)$ is antisymmetric in the neighbourhood of $y = 0$, and so instead of assuming that D_2 is a constant, it is better to write D_2 in the form $A \sin y$ in $(0,\lambda)$, where λ is the value of y at the end of the first interval $(\lambda = \lambda_3)$. Then if D_2 and A_{2k} are redefined by

$$D_2 = A \sin \tfrac{1}{2}\lambda,$$

and

$$A_{2k} = -\frac{1}{\pi \sin \frac{1}{2}\lambda} \int_0^\lambda \sin y^* \log \frac{\sin \frac{1}{2}(y^* - y_k)}{\sin \frac{1}{2}(y^* + y_k)} \, dy^*$$

$$= \frac{1}{\pi \sin \frac{1}{2}\lambda} \left\{ 2 \sin \tfrac{1}{2}(y_k + \lambda) \sin \tfrac{1}{2}(y_k - \lambda) \log \frac{\sin \frac{1}{2}(y_k - \lambda)}{\sin \frac{1}{2}(y_k + \lambda)} + \lambda \sin y_k \right\},$$

equation (14) remains unchanged in form.

Suitable matrices A and B are given in Tables 2 and 3. In these tables $(0,\pi)$ has been subdivided into $(0°,6°,12°,18°,24°,30°,40°, \ldots 160°,170°,180°)$, and y_k has the values $3°,9°,15°,21°,27°,35°,45°, \ldots 165°$ and $175°$. These tables, which are also used for aerofoil design[4], should be quite sufficient for all but the most unusual aerofoil shapes. The interval is reduced near the nose to allow for the greater rate of change in this neighbourhood.

With/

With the definitions of C and D given above, it readily follows from equations (6) that for an aerofoil with only the L.E. and T.E. discontinuities in θ,

$$\int_0^{\pi} C \cos \gamma \, d\gamma = \tau_a - \tau_b$$

$$\int_0^{\pi} C \, d\gamma = \tau_a + \tau_b$$

$$\int_0^{\pi} D \sin \gamma \, d\gamma = 0 .$$

Now a given closed aerofoil does satisfy these equations exactly, but when the aerofoil is replaced by an approximating one for which C and D are constant in small intervals, there results

$$\sum_{i=2}^{n-1} C_i \, [\sin \gamma]_i = \tau_a - \tau_b \qquad \ldots(16)$$

$$\sum_{i=2}^{n-1} C_i \, [\gamma]_i = \tau_a + \tau_b \qquad \ldots(17)$$

$$\sum_{i=2}^{n-1} D_i \, [\cos \gamma]_i = 0, \qquad \ldots(18)$$

(where $[X]_i$ is the jump in X in the i^{th} interval), which are not necessarily satisfied by the given values of τ_a, τ_b and D_i. These equations must be satisfied however, otherwise the approximating aerofoil will not close. This is ensured by using the first two equations to define τ_a and τ_b, completely ignoring the actual values of these angles. The last equation can be satisfied by adjusting the value of D_2.

Now since the values of C_i and D_i in (14) are unknown at the start of the calculation, some iteration is necessary to obtain a solution. If a solution $q/U = q/U(\gamma)$ is assumed, (usually $q/U = 1$), then equation (8) enables $s(\gamma)$, and hence from the given aerofoil co-ordinates, $c/R(\gamma)$, to be calculated. D_i and C_i then follow from their definitions, and equations (16), (17) and (18). Equations (14) and (32) (see p.13 below) then enable $q/U(\gamma)$ to be calculated, thus completing one iteration. A typical example is shown in Table 5, where three iterations proved sufficient to complete the solution.

4./

4. Discussion of the Equation for r: Rules for Calculating C_p from C_{p_o}

The fundamental approximation leading to the solution given by equation (3) is that m can be replaced by m_∞ in the differential equation for r in the (φ,ψ) plane[1]. This is a better approximation than that used in linear perturbation theory, viz., $\beta = \beta_\infty$, for, from the usual compressible flow equations, it can be shown that

$$\beta = \beta_\infty \left\{1 - M_\infty^2 \left(1 + \frac{\upsilon - 1}{2} M_\infty^2\right) \delta/\beta_\infty^2 + O(\delta^2)\right\}, \qquad \ldots(19)$$

$$= \beta_\infty + O(M_\infty^2 \delta),$$

and

$$m = m_\infty \{1 - \tfrac{1}{2}(\upsilon + 1) M_\infty^4 \delta/\beta_\infty^2 + O(\delta^2) \qquad \ldots(20)$$

$$= m_\infty + O(M_\infty^4 \delta),$$

where $\delta = q/U - 1$ and υ is the ratio of the specific heats. The approximation (equation (1)) was first applied by Kármán[6] to the differential equation for ψ in the (r,θ) plane. It leads, in Kármán's analysis, to the conclusion that

$$r \doteq \log(U/q_i) \qquad \ldots(21)$$

where q_i is the velocity of the corresponding incompressible flow about the same aerofoil. Equation (21) can be deduced directly from equations (8) and (13). From (8) it follows that

$$\sigma/c = \int_0^\pi \frac{\sin \gamma}{qc}\, d\gamma,$$

where σ is the semi-perimeter distance. Thus, since σ/c is constant, the mean value of $\sin \gamma/(qc)$ is independent of M_∞. This is also approximately true of the local values of $\sin \gamma/(qc)$, and therefore of the local values of $\sin \gamma/(qR)$. Consequently the right hand side of equation (13) is approximately independent of M_∞, and since from (2) $r = \log(U/q_i)$ when $M_\infty = 0$, equation (21) follows. From equation (11) it follows that approximation (21) is also applicable to an aerofoil at incidence.

Now for reasons he did not give, Kármán used approximation (1) in equation (2) to find

$$r = \int_0^L \frac{m\rho}{\rho_o}\, dL$$

$$\doteq m_\infty \int_0^L \frac{\rho}{\rho_o}\, dL, \qquad \ldots(22)$$

i.e./

i.e.,

$$r = - m_{\infty} \int_0^q \left\{1 - \tfrac{1}{2}(\gamma - 1)\left(\frac{q}{a_o}\right)^2\right\}^{1/(\gamma-1)} \frac{dq}{q},$$

where a_o is the velocity of sound at a stagnation point. By ignoring terms $O(q/a_o)^4$ Kármán then found

$$r = - m_{\infty} \log(q/U) + \frac{U^2}{4a_o^2}\left(1 - \left(\frac{q}{U}\right)^2\right), \tag{23}$$

and so from (21),

$$\left(\frac{q_1}{U}\right)^{1/m_{\infty}} = \frac{q}{U} \exp\{(U^2 - q^2)/4a_o^2\} \tag{24}$$

The well-known Karman-Tsien result, viz.,[6]

$$C_p = \frac{1}{\beta_\infty} \frac{C_{p_o}}{1 + \dfrac{1 - \beta_\infty}{2\beta_\infty} C_{p_o}},$$

$$\text{or} \qquad C_p = \frac{1}{\beta} C_{p_o} - \frac{1 - \beta_\infty}{2\beta_\infty^2} C_{p_o}^2 + O(C_{p_o})^3, \tag{25}$$

also follows directly from (21) and (22). This may be shown as follows. It is easily established that

$$\frac{\rho}{\rho_o} = \frac{\rho_\infty}{\rho_o}\{1 - M_\infty^2 \delta + O(\delta^2)\},$$

$$\text{and} \qquad \delta = -\tfrac{1}{2}C_p\{1 + \tfrac{1}{4}\beta_\infty^2 C_p\} + O(C_p^3), \tag{26}$$

thus from (22) and (26)

$$\sim \; = \tfrac{1}{2}\beta_\infty C_p\{1 + \tfrac{1}{2}C_p\} + O(C_p^3) \tag{27}$$

From equation (21)

$$r = \log(U/q_1) = -\tfrac{1}{2}\log(1 - C_{p_o}) = \tfrac{1}{2}C_{p_o}\{1 + \tfrac{1}{2}C_{p_o}\} + O(C_{p_o}^3) \tag{28}$$

equation (25) now follows from equations (27) and (28).

While/

While perhaps it may be "consistent" to use approximation (1) in deriving equation (22), it is unnecessary, as equation (2) can be integrated directly to yield

$$r = \frac{\sqrt{6}}{2} \log \left| \frac{\sqrt{6} - \beta}{\sqrt{6} - \beta_\infty} \frac{\sqrt{6} + \beta_\infty}{\sqrt{6} + \beta} \right| + \tfrac{1}{2} \log \left| \frac{1 - \beta_\infty}{1 - \beta} \frac{1 + \beta}{1 + \beta_\infty} \right| ,$$

or in terms of C_p (use (19) and (26)),

$$r = \tfrac{1}{2}\beta_\infty C_p \left\{ 1 + \tfrac{1}{2}C_p \left(1 + \frac{\nu + 1}{4} \frac{M_\infty^4}{\beta_\infty^2} \right) \right\} + O(C_p^3) .$$

From (28) it then follows that

$$C_p = \frac{1}{\beta_\infty} C_{p_0} - \frac{1}{2\beta_\infty^2} \left(1 - \beta_\infty + \frac{(\nu + 1)}{4} \frac{M_\infty^4}{\beta_\infty^2} \right) C_{p_0}^2 + O(C_{p_0}^3) . \qquad \ldots(29)$$

Equations (24) and (25) lead to very similar results, as they are both derived from equations (21) and (22); some comparison is made between them in reference 6. Apart from the above mentioned "consistency", which appears to have no more than a formal significance, there are no theoretical grounds for preferring equation (25) over equation (29). The additional term in equation (29) roughly doubles the coefficient of $C_{p_0}^2$ at $M_\infty = 0.7$. For the example shown in figure 12b of reference 6 equation (29) would clearly give much closer agreement with experiment than equation (25), but the author has found that in a number of cases the experimental values of C_p lie between the results calculated from (25) and (29). Figures 2 and 3 illustrate this point.

The curve shown in figure 3, due to Laitone, and introduced only because it has been published recently without discussion of its merit, was calculated from[7]

$$C_p = \frac{1}{\beta_\infty} C_{p_0} - \frac{2M_\infty^2 + (\nu - 1)M_\infty^4}{4\beta_\infty^4} C_{p_0}^2 .$$

It is clear from the figure that this equation is of little value.

The experimental evidence suggests replacing equation (2) by the average of equations (2) and (22), i.e., by

$$r = \int_0^L \tfrac{1}{2}(m + m_\infty) \frac{\rho}{\rho_0} \, dL , \qquad \ldots(30)$$

and/

and this will be done in the remainder of this paper. Equation (29) then becomes

$$C_p = \frac{1}{\beta_\infty} C_{p_0} - \frac{1}{2\beta_\infty^2}\left(1 - \beta_\infty + \frac{(\upsilon + 1)}{8}\frac{M_\infty^4}{\beta_\infty^2}\right) + O(C_{p_0}^3). \qquad \ldots(31)$$

Equation (31) is thus "semi-empirical", but no more so than equation (24). Although (30) can be integrated exactly it is quicker in practice to use numerical methods to obtain the relation

$$r = r\left(\frac{q}{U}\right), \qquad \ldots(32)$$

which is set out in Table 1 for $M_\infty = 0.5, 0.7$ and 0.79. A small supersonic patch was experienced when calculating (32) at $M_\infty = 0.79$. For this region β was redefined empirically to be $(M_\infty^2 - 1)^{\frac{1}{2}}$.

5. Calculation of Lift and Moment Coefficients and their Rates of Change with Incidence

The lift coefficient is defined by the contour integral

$$C_L = -\frac{1}{c}\oint C_p \cos\theta \, ds,$$

where c is the aerofoil chord. Thus, since

$$\frac{1}{c}\cos\theta\, ds = \frac{\cos\theta}{c\,q}\,d\phi = \left(\frac{2a}{Uc}\right)\sin\gamma\left(\frac{U\cos\theta}{q}\right)d\gamma,$$

$$C_L = -\left(\frac{2a}{Uc}\right)\int_{-\pi}^{\pi} C_p \sin\gamma\left(\frac{U\cos\theta}{q}\right)d\gamma. \qquad \ldots(33)$$

In this expression $\left(\dfrac{U\cos\theta}{q}\right)$ can readily be deduced as a function of γ when the zero incidence solution has been calculated by the method of section 3, while C_p, which is a function of γ and α, can be calculated by using (11) and (32) to determine (q_α/U), and then

$$C_p = \frac{2}{\upsilon M_\infty^2}\left\{\left[1 - \frac{\upsilon - 1}{2}M_\infty^2\left\{\left(\frac{q_\alpha}{U}\right)^2 - 1\right\}\right]^{\upsilon/(\upsilon-1)} - 1\right\}. \qquad \ldots(34)$$

Similarly/

Similarly the equation

$$C_M = \left(\frac{2a}{Uc}\right) \int_{-\pi}^{\pi} C_p \left(\frac{x}{c} \cos\theta + \frac{y}{c} \sin\theta\right) \frac{U}{q} \sin\gamma \, d\gamma, \qquad \ldots(35)$$

enables the moment coefficient about the leading edge to be calculated.

From equations (11) and (30) it follows that

$$\frac{\partial(q_\alpha/U)}{\partial\alpha} = \frac{2m_\infty}{\beta_\infty(m_\infty + m)} \frac{q_\alpha}{U} \frac{\rho_\infty}{\rho} \cot(\tfrac{1}{2}\gamma + \alpha),$$

and since from (34) it can be deduced that

$$\frac{\partial C_p}{\partial(q_\alpha/U)} = -2 \frac{q_\alpha}{U} \frac{\rho}{\rho_\infty},$$

then

$$\frac{\partial C_p}{\partial\alpha} = -\frac{2}{\beta_\infty} \left(\frac{2m_\infty}{m_\infty + m}\right) \left(\frac{q_\alpha}{U}\right)^2 \cot(\tfrac{1}{2}\gamma + \alpha).$$

Thus differentiation of (33) and (35) with respect to α yields

$$\frac{\partial C_L}{\partial\alpha} = \frac{1}{\beta_\infty} \left(\frac{4a}{Uc}\right) \int_{-\pi}^{\pi} \left(\frac{2m_\infty}{m_\infty + m}\right) \left(\frac{q_\alpha}{U}\right)^2 \left(\frac{U}{q} \cos\theta\right) \sin\gamma \cot(\tfrac{1}{2}\gamma + \alpha) \, d\gamma, \qquad \ldots(36)$$

and

$$\frac{\partial C_M}{\partial\alpha} = \frac{1}{\beta_\infty} \left(\frac{4a}{Uc}\right) \int_{-\pi}^{\pi} \left(\frac{2m_\infty}{m_\infty + m}\right) \left(\frac{q_\alpha}{U}\right)^2 \left(\frac{U}{q}\right) \left(\frac{x}{c} \cos\theta + \frac{y}{c} \sin\theta\right) \sin\gamma \cot(\tfrac{1}{2}\gamma + \alpha) \, d\gamma. \qquad \ldots(37)$$

The function

$$\chi\left(\frac{q_\alpha}{U}\right) \equiv \left(\frac{2m_\infty}{m_\infty + m}\right)$$

is given in Table 1 for M_∞ = 0.5, 0.7 and 0.79.

For/

For a symmetrical aerofoil at zero incidence equations (36) and (37) reduce to

$$\frac{\partial C_L}{\partial \alpha} = \frac{4}{\beta_\infty}\left(\frac{4a}{Uc}\right)\int_0^\pi \left(\frac{2n_\infty}{n_\infty + n}\right)\left(\frac{q}{U}\cos\theta\right)\cos^2 \tfrac{1}{2}y \, dy, \qquad \ldots(38)$$

and

$$\frac{\partial C_M}{\partial \alpha} = \frac{4}{\beta_\infty}\left(\frac{4a}{Uc}\right)\int_0^\pi \left(\frac{2n_\infty}{n_\infty + n}\right)\left(\frac{q}{U}\right)\left(\frac{x}{c}\cos\theta + \frac{y}{c}\sin\theta\right)\cos^2 \tfrac{1}{2}y \, dy. \qquad \ldots(39)$$

For thin aerofoils (38) yields approximately

$$\frac{\partial C_L}{\partial \alpha} = \frac{2\pi}{\beta_\infty}\left(\frac{4a}{Uc}\right),$$

which is the result given by linear perturbation theory.

6. An Example: Aerofoil R.A.E.104

The co-ordinates[8] and various derived functions for this symmetrical aerofoil are set out in Table 4. Column 4 is the difference between the perimeter distance and the x co-ordinate, both measured from the leading edge.

The calculation of the incompressible flow at zero incidence is set out in full in Table 5, the columns of which will now be discussed. The assumption

$$q = U, \qquad \ldots(40)$$

is equivalent to assuming that the aerofoil is a flat plate, i.e., $s = x$. Equation (8) then yields

$$\frac{xU}{2a} = 1 - \cos y, \quad \frac{cU}{2a} = 1 - \cos\pi = 2, \qquad \ldots(41)$$

and so

$$\frac{x}{c} = \tfrac{1}{2}(1 - \cos y),$$

from which column 1 is obtained. This column will, of course, be the same for all aerofoil shapes. Since the aerofoil is symmetrical, from equations (15), (40) and (41), $D_i = 0$, and $C_i = \tfrac{1}{2}(c/R)\sin y$.

"c/R"/

"c/R" is obtained from Table 4, or from a graph, c/R v. x/c. The first and last entries in column 2 are $-\tau_a$ and $-\tau_b$, which must be calculated by using the remainder of column 2 in equations (16) and (17). Column 20, Table 5 is of assistance in this calculation; $[\gamma]_i$ is 0.1045 rad. (6°) up to $\gamma = 27°$, and 0.1745 rad. (10°) for $\gamma > 27°$. Column 3 follows from column 2 and Table 3 - see equations (2) and (14), while the derivation of columns 4 and 5 is obvious. Column 6 is obtained by integrating column 5 (see equation (8)). From the last entries in column 4, Table 4 and column 6, Table 5, it follows that

$$\frac{2a}{Uc} = \frac{1.0117}{1.8798} = 0.5382, \qquad \ldots(42)$$

and hence if column 6 is multiplied by this number, column 7 results. Column 8, which is derived from column 4, Table 4 and column 7, Table 5, completes one iteration. From equations (15) and (42)

$$C_i = 0.5382\left(\frac{c}{R}\right)\left(\frac{U}{q}\sin\gamma\right),$$

which can be calculated from column 5, Table 5 and Table 4. The calculation now proceeds through the next iteration in an obvious way. The final solution is given by columns 15 and 18. Column 19 gives the values of q_1/U given in reference 8 and calculated by Goldstein's Approximation III.

The only difference in the compressible flow calculations is that $\log(U/q_i)$ is replaced by r and therefore logarithm tables are replaced by tables like Table 1. A good approximation to start the iteration is $r = \log(U/q_i)$ (equation (21)), and so column 17 of Table 5 becomes the first column (labelled r) of the compressible flow calculation. If this is done one iteration is usually sufficient. A further point is that, in view of the inaccuracy of equation (1) near stagnation points, it is sufficient to take the entries for $\gamma = 3°$ from the last iteration of the incompressible flow calculation. The solution at $M = 0.7$ is given in Table 6.

Also shown in Table 6 is the scheme of calculation of $\partial C_L/\partial\alpha$ and $\partial C_M/\partial\alpha$, at $M_\infty = 0.7$, $\alpha = 0$. In this table column 4 is derived from column 1, column 5 from column 3 and Table 4, column 6 from column 3 and Table 1, while column 8 is obtained from column 2 and Table 4. The integrals of columns 7 and 9 are shown in the table. Then from equations (38) and (39) it follows that

$$\frac{\partial C_L}{\partial\alpha} = \frac{4}{\beta_\infty}\left(\frac{4a}{Uc}\right) \times 1.7367 = \frac{4}{0.7141} \times 1.1200 \times 1.7367 = 10.895,$$

and

$$\frac{\partial C_M}{\partial\alpha} = \frac{4}{\beta_\infty}\left(\frac{4a}{Uc}\right) \times 0.4565 = 2.864.$$

Thus/

Thus $$\frac{\partial C_M}{\partial C_L} = \frac{2.864}{10.895} = 0.263 .$$

The results for $M_{\infty} = 0$, 0.7 and 0.79 are set outin Table 7. The experimental results given in this table are taken from Figures 8, 9 and 10 of reference 9. All that can be concluded from these results is that for aerofoil R.A.E.104 $\left(\frac{\partial^2 C_L}{\partial\alpha\partial M_{\infty}}\right)_{exp.}$ lies between the value given by linear perturbation theory and that given by equation (38). It appears from Figures 8, 9 and 10 of reference 9 that boundary layer effects are very complex for this aerofoil.

Figures 4 and 5 show the theoretical and experimental velocity distributions at $M = 0$ and 0.7. A comparison has been made between the theoretical and experimental values at approximately the same values of C_L. The satisfactory agreement indicates that it is the circulation (or position of the front stagnation point) rather than the incidence, that determines the velocity distribution over the front half of an aerofoil.

It will be noticed from Figure 5 that the theory overestimates the values of q/U, particularly near the nose. It appears from the figure that if this error could be eliminated from the zero incidence result the error in the results at incidence would be largely eliminated. In other words, provided that the comparisons are made at the same values of C_L, equation (11) (giving the incidence contribution) is more accurate at high Mach numbers than equation (10) (giving the thickness contribution).

7. Acknowledgement

The calculations for this paper were made by Miss E. M. Tingle of the Aerodynamics Division, N.P.L.

References

No.	Author(s)	Title, etc.
1.	L. C. Woods	The two-dimensional subsonic flow of an inviscid fluid about an aerofoil of arbitrary shape (combining A.R.C.'s 13,240, 13,395, 13,460 and 13,533) to be published as R. & M.2811.
2.	S. Goldstein	A theory of aerofoils of small thickness. Parts I - VI. C.P. Nos. 68, 69, 70, 71, 72 and 73.
3	L. C. Woods	Compressible subsonic flow in two-dimensional channels: The direct and indirect problems. A.R.C.14,838.
4.	L. C. Woods	Aerofoil design in two-dimensional subsonic compressible flow. R. & M. 2845. March, 1952.

References (Continued)

No.	Author(s)	Title, etc.
5.	M. B. Glauert.	The application of the exact method of aerofoil design. R. & M. 2683. October, 1947.
6.	Th. von Kármán.	Compressibility effects in aerodynamics. Jour. Aero. Sci., Vol.8, No.9, July, 1941.
7.	E. V. Laitone.	Jour. Aero. Sci., Vol.18, No.12, December, 1951.
8.	R. C. Pankhurst and H. B. Squire.	Calculated pressure distributions for the R.A.E. 100-104 aerofoils sections. C.P. No. 80. March, 1950.
9.	E. W. E. Rogers, C. J. Berry and R. F. Cash.	Tests at high subsonic speeds on a 10% thick pressure-plotting aerofoil of R.A.E. 104 section. Part I - Force coefficients. R. & M. 2863. November, 1950.
10.	L. C. Woods.	The second order terms in two-dimensional channel blockage. (A revised version of A.R.C. 13,663.) To be published in the Aero. Quart.
11.	M. J. Lighthill.	A new method of two-dimensional aerodynamic design. R. & M. 2112. April, 1945.
12.	L. M. Milne-Thomson.	Theoretical hydrodynamics. Macmillan & Co., 1949.

/TABLE 1

TABLE 1

$$r = r(q/U), \quad \chi = \frac{2n_{\infty}}{n_{\infty} + n}$$

	$M_\infty = 0.5$		$M_\infty = 0.7$		$M_\infty = 0.79$	
q/U	$r \times 10^4$	χ	$r \times 10^4$	χ	$r \times 10^4$	χ
0.72	2956	0.992	2573	0.959	2314	0.919
0.76	2457	0.992	2125	0.962	1901	0.925
0.80	1988	0.993	1707	0.965	1519	0.931
0.84	1545	0.994	1317	0.970	1165	0.939
0.88	1126	0.995	953	0.975	838	0.949
0.92	731	0.997	613	0.982	535	0.962
0.96	355	0.998	296	0.990	256	0.978
1.00	0	1.000	0	1.000	0	1.000
1.00	0	1.000	0	1.000	0	1.000
1.02	-171	1.001	-140	1.006	-120	1.013
1.04	-335	1.002	-276	1.013	-235	1.029
1.06	-500	1.003	-406	1.021	-343	1.047
1.08	-658	1.005	-532	1.029	-447	1.069
1.10	-813	1.006	-653	1.038	-543	1.095
1.12	-963	1.008	-770	1.049	-637	1.128
1.14	-1110	1.009	-882	1.061	-724	1.169
1.16	-1253	1.011	-989	1.076	-804	1.222
1.18	-1392	1.013	-1092	1.092	-879	1.296
1.20	-1528	1.015	-1190	1.110	-946	1.412
1.22	-1661	1.017	-1284	1.133	-1001	1.669
1.24	-1791	1.020	-1373	1.159	-1054	1.505
1.26	-1917	1.022	-1457	1.192	-1112	1.316
1.28	-2040	1.025	-1537	1.232	-1175	1.198
1.30	-2161	1.028	-1611	1.284	-1241	1.110

TABLE 2/

TABLE 2: A × 10^4

γ	3	9	15	21	27	35	45	55	65	75
3	361	284	160	128	98	74	57	45	37	31
9	242	928	474	305	228	171	128	102	83	69
15	136	474	1097	607	414	298	220	173	140	116
21	96	305	607	1205	698	452	322	249	200	164
27	73	228	414	698	1284	675	443	333	265	216
35	93	286	499	761	1152	1986	1135	786	605	487
45	71	215	368	539	742	1135	2103	1232	868	673
55	56	170	288	415	557	786	1232	2185	1301	924
65	46	138	234	334	442	605	868	1301	2241	1346
75	38	115	193	274	361	487	673	924	1346	2276
85	32	96	161	228	299	399	543	719	959	1372
95	27	80	135	191	249	331	445	578	745	976
105	22	67	113	159	207	275	366	471	595	753
115	19	56	94	132	171	227	301	384	479	595
125	15	46	76	108	140	184	244	309	384	471
135	12	36	61	86	111	146	193	244	301	366
145	9	28	46	65	84	111	146	184	227	275
155	7	19	33	46	59	78	102	129	158	191
165	4	12	19	27	35	46	61	76	94	113
175	1	4	6	9	12	15	20	25	31	37

	85	95	105	115	125	135	145	155	165	175
3	26	20	19	15	13	10	8	6	4	0
9	57	48	40	34	27	22	17	12	7	2
15	97	81	68	56	46	36	28	20	12	4
21	137	114	96	79	65	51	39	27	16	5
27	179	149	124	103	84	67	51	36	21	7
35	399	331	275	227	184	146	111	78	46	15
45	543	445	366	301	244	192	146	102	61	20
55	719	578	471	384	309	244	184	129	76	25
65	959	745	595	479	384	301	227	158	94	31
75	1372	976	753	595	471	366	275	191	113	37
85	2293	1381	976	745	578	445	331	229	135	45
95	1381	2293	1372	959	719	543	399	275	161	53
105	976	1372	2276	1346	924	673	487	331	193	63
115	745	959	1346	2241	1301	868	605	405	234	76
125	578	719	924	1301	2185	1232	786	508	288	94
135	445	543	673	868	1232	2103	1135	669	368	118
145	331	399	487	605	786	1135	1986	995	499	156
155	229	275	331	405	508	669	995	1816	783	225
165	135	161	193	234	288	368	499	783	1542	402
175	45	53	63	76	94	118	156	225	402	915

TABLE 3: $B \times 10^4$

Y	0	3	9	15	21	27	35	45	55	65	75
0	-	23191	16203	12963	10838	9262	7650	6115	4919	3955	3160
3	2633	2546	1755	1376	1144	976	805	643	517	415	332
9	1710	1755	2168	1523	1207	1012	826	655	525	422	337
15	1362	1376	1523	1999	1390	1099	872	682	543	435	347
21	1137	1144	1207	1390	1890	1299	956	727	572	455	362
27	971	976	1012	1099	1299	1811	1117	797	614	484	384
35	1339	1343	1379	1458	1603	1890	2605	1627	1172	902	709
45	1070	1072	1094	1139	1215	1334	1627	2489	1529	1090	834
55	860	862	877	907	955	1026	1172	1529	2407	1461	1034
65	691	693	704	725	760	809	902	1090	1461	2351	1416
75	553	554	562	579	605	641	709	834	1034	1416	2315
85	436	437	444	458	479	507	560	652	788	998	1390
95	339	340	346	357	374	398	441	514	617	762	981
105	258	258	263	273	288	308	344	405	488	600	754
115	190	190	195	203	216	234	265	318	388	480	600
125	134	134	138	146	158	174	202	248	310	388	488
135	88	89	92	100	111	125	151	193	249	318	405
145	53	54	57	64	74	87	111	151	202	265	344
155	27	27	31	37	47	60	82	120	168	228	301
165	10	10	13	20	29	42	64	100	146	203	273
175	1	2	5	11	20	33	54	90	135	191	260
180	-	2	19	55	107	178	302	504	763	1084	1474

Y	85	95	105	115	125	135	145	155	165	175	180
0	2497	1940	1474	1084	763	504	302	153	55	6	-
3	262	204	155	114	80	53	32	16	6	0	0
9	266	207	158	117	83	55	34	18	8	3	2
15	274	214	164	122	87	60	38	22	12	7	6
21	287	224	173	130	94	66	44	28	17	12	11
27	304	239	185	140	104	75	52	36	25	19	19
35	560	441	344	265	202	151	111	82	64	54	53
45	652	514	405	318	248	193	151	120	100	90	88
55	788	617	488	388	310	248	202	168	146	135	134
65	998	762	600	480	388	318	265	228	203	191	190
75	1390	981	754	600	488	405	344	301	273	260	258
85	2298	1381	981	762	617	514	441	390	357	341	339
95	1381	2298	1390	998	788	652	560	497	458	439	436
105	981	1390	2315	1416	1034	834	709	628	579	555	553
115	762	998	1416	2351	1461	1090	902	791	726	695	691
125	617	788	1034	1461	2407	1529	1172	1000	907	865	860
135	514	652	834	1090	1529	2489	1627	1288	1139	1077	1070
145	441	560	709	902	1172	1627	2605	1767	1458	1351	1339
155	390	497	628	791	1000	1288	1767	2775	1978	1732	1708
165	357	458	579	726	907	1139	1458	1978	3049	2359	2284
175	341	439	555	695	865	1077	1351	1732	2359	3676	3821
180	1940	2497	3160	3955	4919	6155	7650	9743	12963	19941	-

TABLE 4/

TABLE 4: Co-ordinates of R.A.E.104

1	2	3	4	5	6	1	2	3	4	5	6
10^3 x/c	10^3 y/c	c/R	s - x	cos θ	x/c (1 + y/x tan θ)	10^3 x/c	10^3 y/c	c/R	s - x	cos θ	x/c (1 + y/x tan θ)
0	0	168	0		0	320	48.556	0.31	9.3	1.000	0.3215
1	3.441	112	2.6	0.381	0.0094	340	49.082	0.30	"		
2	4.863	79	3.0	0.633	0.0079	360	49.488	0.30	"	1.000	0.3609
3	5.953	61.1	3.6	0.706	0.0089	380	49.775		"		
4	6.870	48.0	4.0	0.755	0.0100	400	49.946		"	1.000	0.4000
5	7.676	39.0	4.3	0.792	0.0109	420	50.000	0.29	"		
6	8.404		4.6	0.819	0.0119	440	49.937	0.29	"	1.000	0.4400
7	9.072	27.1	4.8	0.842	0.0128	460	49.756		"		
8	9.692		5.0	0.857	0.0138	480	49.454	0.31	"	1.000	0.4809
9	10.274	21.2	5.2	0.870	0.0148	500	49.027		"		
10	10.824		5.4			520	48.468	0.35	"	1.000	0.5215
12	11.842	15.3	5.6	0.902	0.0176	540	47.769		"		
14	12.776	12.9	5.8	0.911	0.0198	560	46.917	0.43	"	0.999	0.5622
16	13.642		6.0	0.926	0.0215	580	45.892	0.54	"		
18	14.452	9.54	6.2	0.930	0.0236	600	44.650	0.74	9.3	0.998	0.6031
20	15.215		6.4			620	43.113	0.51	9.4		
25	16.960	6.28	6.6	0.949	0.0306	640	41.370	0.38	9.5	0.996	0.6438
30	18.522	4.88	6.9			660	39.473	0.31	9.6		
35	19.945	4.08	7.1	0.964	0.0405	680	37.452	0.25	9.7	0.995	0.6839
40	21.256		7.3			700	35.331	0.21	9.8		
50	23.617	2.50	7.5	0.976	0.0553	720	33.128	0.16	9.9	0.994	0.7237
60	25.709	1.98	7.8			740	30.861	0.12	10.0		
70	27.592		8.1	0.985	0.0749	760	28.545	0.09	10.2	0.993	0.7633
80	29.307		8.3			780	26.193	0.05	10.3		
90	30.881	1.14	8.5	0.989	0.0947	800	23.819	0.05	10.4	0.993	0.8028
			8.6								

TABLE 4 (Contd.)/

TABLE 4 (Contd.): Co-ordinates of R.A.E.104

1	2	3	4	5	6	1	2	3	4	5	6
10^3 x/c	10^3 y/c	c/R	s - x	cos θ	x/c (1 + y/x tan θ)	10^3 x/c	10^3 y/c	c/R	s - x	cos θ	x/c (1 + y/x tan θ)
100	32.336		8.7			820	21.437	0	10.6		
120	34.945	0.81	8.9	0.993	0.1242	840	19.055	0	10.7	0.993	0.8423
140	37.222	0.68	9.0			860	16.673	0	10.9		
160	39.224		9.1	0.996	0.1637	880	14.292	0	11.0	0.993	0.8817
180	40.992	0.51	9.2			900	11.910	0	11.2		
200	42.556	0.46	9.3	0.997	0.2031	920	9.528	0	11.3	0.993	0.9211
220	43.936	0.42	9.3			940	7.146	0	11.4		
240	45.149	0.38	"	0.998	0.2426	960	4.764	0	11.6	0.993	0.9606
260	46.208	0.36	"			980	2.382	0	11.7		
280	47.124	0.34	"	0.999	0.2820	1000	0	-		0.994	1.0000
300	47.905	0.32	9.3								

TABLE 5/

TABLE 5: Calculation of Incompressible Flow about R.A.E.104

	1	2	3	4	5	6	7	8	9	10	11
$\gamma_{i+\frac{1}{2}}$	x/c	C_i	log U/q	q/U	U/q sin γ	s/c/(2a/Jc)	s/c	x/c	C_i	log U/q	q/U
0	0	-1.0461	∞	0	-	0	0	0	-1.5411	∞	0
3	0.0007	3.270	0.7298	0.482	0.108	0.0047	0.0025	0.0008	7.020	0.7705	0.463
9	0.0062	2.410	0.1293	0.879	0.178	0.0197	0.0106	0.0059	3.090	0.0899	0.914
15	0.0175	1.330	-0.0170	1.017	0.255	0.0423	0.0227	0.0165	1.485	-0.0394	1.040
21	0.0333	0.772	-0.0637	1.066	0.336	0.0732	0.0393	0.0321	0.817	-0.0761	1.079
27	0.0545	0.518	-0.0836	1.088	0.418	0.1127	0.061	0.053	0.528	-0.0918	1.096
35	0.0905	0.316	-0.0938	1.098	0.523	0.1789	0.096	0.087	0.325	-0.1008	1.106
45	0.147	0.209	-0.1011	1.107	0.639	0.2802	0.151	0.142	0.229	-0.1090	1.115
55	0.213	0.176	-0.1069	1.113	0.735	0.3582	0.193	0.184	0.197	-0.1143	1.121
65	0.288	0.151	-0.1096	1.116	0.813	0.5357	0.288	0.279	0.149	-0.1139	1.121
75	0.370	0.142	-0.1111	1.118	0.865	0.6819	0.367	0.358	0.138	-0.1142	1.121
85	0.457	0.149	-0.1111	1.118	0.892	0.8350	0.449	0.440	0.141	-0.1136	1.120
95	0.543	0.196	-0.1101	1.117	0.892	0.9907	0.533	0.524	0.170	-0.1136	1.120
105	0.628	0.215	-0.0970	1.102	0.877	1.1487	0.618	0.609	0.276	-0.1093	1.116
115	0.711	0.080	-0.0624	1.064	0.852	1.2986	0.699	0.689	0.103	-0.0722	1.075
125	0.787	0.017	-0.0289	1.029	0.796	1.4423	0.776	0.766	0.033	-0.0353	1.036
135	0.854	0	-0.0005	1.001	0.706	1.5733	0.847	0.836	0	-0.0025	1.003
145	0.910	0	0.0248	0.976	0.588	1.6874	0.908	0.897	0	0.0260	0.974
155	0.953	0	0.0538	0.948	0.447	1.7777	0.957	0.946	0	0.0582	0.944
165	0.983	0	0.0925	0.922	0.277	1.8415	0.991	0.979	0	0.1008	0.904
175	0.998	0	0.1712	0.843	0.103	1.8746	1.009	0.997	0	0.1878	0.829
180	1.000	-0.1100	∞	0	0	1.8798	1.012	1.000	-0.1210	∞	0

TABLE 5 (Contd.)/

TABLE 5 (Contd.): Calculation of Incompressible Flow about R.A.E.104

	12	13	14	15	16	17	18	19	20	21
	U/q sin y	s/c/(2c/Uc)	s/c	x/c	C_i	log U/q	q/U	q/U	$[\sin y]_i$	$[-\cos y]_i$
0	-	0	0	0	-1.5215	∞	0	0		
3	0.113	0.0051	0.0028	0.0008	7.020	0.7548	0.470	-	0.1045	0.0055
9	0.171	0.0200	0.0108	0.0060	2.950	0.0942	0.910	0.914	0.1034	0.0164
15	0.249	0.0420	0.0227	0.0165	1.455	-0.0364	1.037	1.035	0.1011	0.0271
21	0.333	0.0724	0.0391	0.0319	0.822	-0.0754	1.078	1.074	0.0977	0.0376
27	0.414	0.1115	0.060	0.053	0.528	-0.0911	1.095	1.093	0.0933	0.0475
35	0.518	0.1769	0.096	0.088	0.323	-0.0997	1.105	1.105	0.1428	0.1000
45	0.634	0.2774	0.150	0.141	0.231	-0.1074	1.113	1.112	0.1232	0.1232
55	0.731	0.3965	0.215	0.206	0.176	-0.1106	1.117	1.115	0.1000	0.1428
65	0.810	0.5308	0.287	0.279	0.149	-0.1120	1.119	1.117	0.0737	0.1580
75	0.862	0.6782	0.367	0.358	0.138	-0.1132	1.120	1.118	0.0451	0.1684
85	0.889	0.8310	0.449	0.440	0.141	-0.1131	1.120	1.118	0.0152	0.1736
95	0.889	0.9861	0.533	0.524	0.170	-0.1137	1.120	1.118	-0.0152	0.1736
105	0.865	1.1391	0.616	0.607	0.281	-0.1101	1.117	1.114	-0.0451	0.1684
115	0.844	1.2900	0.697	0.687	0.105	-0.0729	1.075	1.074	-0.0737	0.1580
125	0.792	1.4327	0.775	0.765	0.034	-0.0358	1.037	1.035	-0.1000	0.1428
135	0.705	1.5633	0.845	0.834	0	-0.0028	1.003	1.001	-0.1232	0.1232
145	0.589	1.6762	0.906	0.895	0	0.0257	0.975	0.974	-0.1428	0.1000
155	0.448	1.7683	0.956	0.945	0	0.0580	0.944	0.950	-0.1580	0.0737
165	0.266	1.8323	0.991	0.979	0	0.1006	0.904	-	-0.1684	0.0451
175	0.105	1.8664	1.009	0.997	0	0.1876	0.829	-	-0.1736	0.0152
180	0	1.8716	1.012	1.000	-0.1210	∞	0	0		

TABLE 6/

TABLE 6: Calculation of $\partial C_L/\partial\alpha$, $\partial C_D/\partial\alpha$ at M_∞ = 0.7

1	2	3	4	5	6	7	8	9
y	Solution at M_∞ = 0.70: x/c	q/U	A = $\cos^2 y/2$	B = $q/U \cos\theta$	C = χ	A x B x C	D = $x/c\ \{1 + y/x\ dy/dx\}$	A x B x C x D
0	0	0	1.000	0	-	0	0	0
3	0.0008	0.470	1.000	0.141	0.949	0.134	0.007	0.001
9	0.0067	0.883	0.994	0.737	0.975	0.714	0.013	0.009
15	0.0177	1.051	0.981	0.977	1.017	0.975	0.024	0.023
21	0.0337	1.110	0.964	1.070	1.044	1.077	0.037	0.040
27	0.054	1.139	0.944	1.114	1.061	1.116	0.060	0.067
35	0.087	1.156	0.909	1.142	1.073	1.114	0.090	0.100
45	0.140	1.176	0.852	1.165	1.084	1.076	0.144	0.155
55	0.204	1.178	0.785	1.174	1.090	1.005	0.207	0.208
65	0.275	1.180	0.710	1.179	1.092	0.914	0.277	0.253
75	0.352	1.181	0.629	1.181	1.093	0.812	0.351	0.285
85	0.433	1.179	0.543	1.179	1.091	0.698	0.430	0.300
95	0.516	1.178	0.458	1.178	1.090	0.588	0.510	0.300
105	0.597	1.167	0.371	1.165	1.082	0.468	0.603	0.282
115	0.676	1.110	0.288	1.104	1.044	0.332	0.679	0.225
125	0.755	1.053	0.214	1.046	1.018	0.229	0.758	0.174
135	0.827	1.005	0.147	0.998	1.002	0.147	0.827	0.122
145	0.889	0.967	0.091	0.960	0.992	0.087	0.889	0.077
155	0.941	0.927	0.047	0.921	0.983	0.043	0.941	0.040
165	0.977	0.878	0.017	0.872	0.975	0.014	0.977	0.014
175	0.997	0.790	0.002	0.784	0.965	0.002	0.997	0.002
180	1.000	0	0	0	-	0	1.000	0
	$2a/Uc$ =	0.5600				$\int$ = 1.7367		$\int$ = 0.4565

TABLE 7/

TABLE 7: Values of $\partial C_L/\partial\alpha$, $\partial C_m/\partial\alpha$ and $\partial C_m/\partial C_L$

	M_∞	0	0.7	0.79
Theoretical	$\frac{\partial C_L}{\partial\alpha}$	6.780	10.895	17.473
	$\frac{\partial C_m}{\partial\alpha}$	1.809	2.864	4.512
	$\frac{\partial C_m}{\partial C_L}$	0.267	0.263	0.258
Linear Perturbation	$\frac{\partial C_L}{\partial\alpha}$	6.780	9.494	11.058
	$\frac{\partial C_m}{\partial\alpha}$	1.809	2.533	2.951
	$\frac{\partial C_m}{\partial C_L}$	0.267	0.267	0.267
Experimental	$\frac{\partial C_L}{\partial\alpha}$	5.7	8.5	10.9
	$\frac{\partial C_m}{\partial\alpha}$	1.7	2.5	3.1
	$\frac{\partial C_m}{\partial C_L}$	0.29	0.29	0.28

KM.

FIG 2

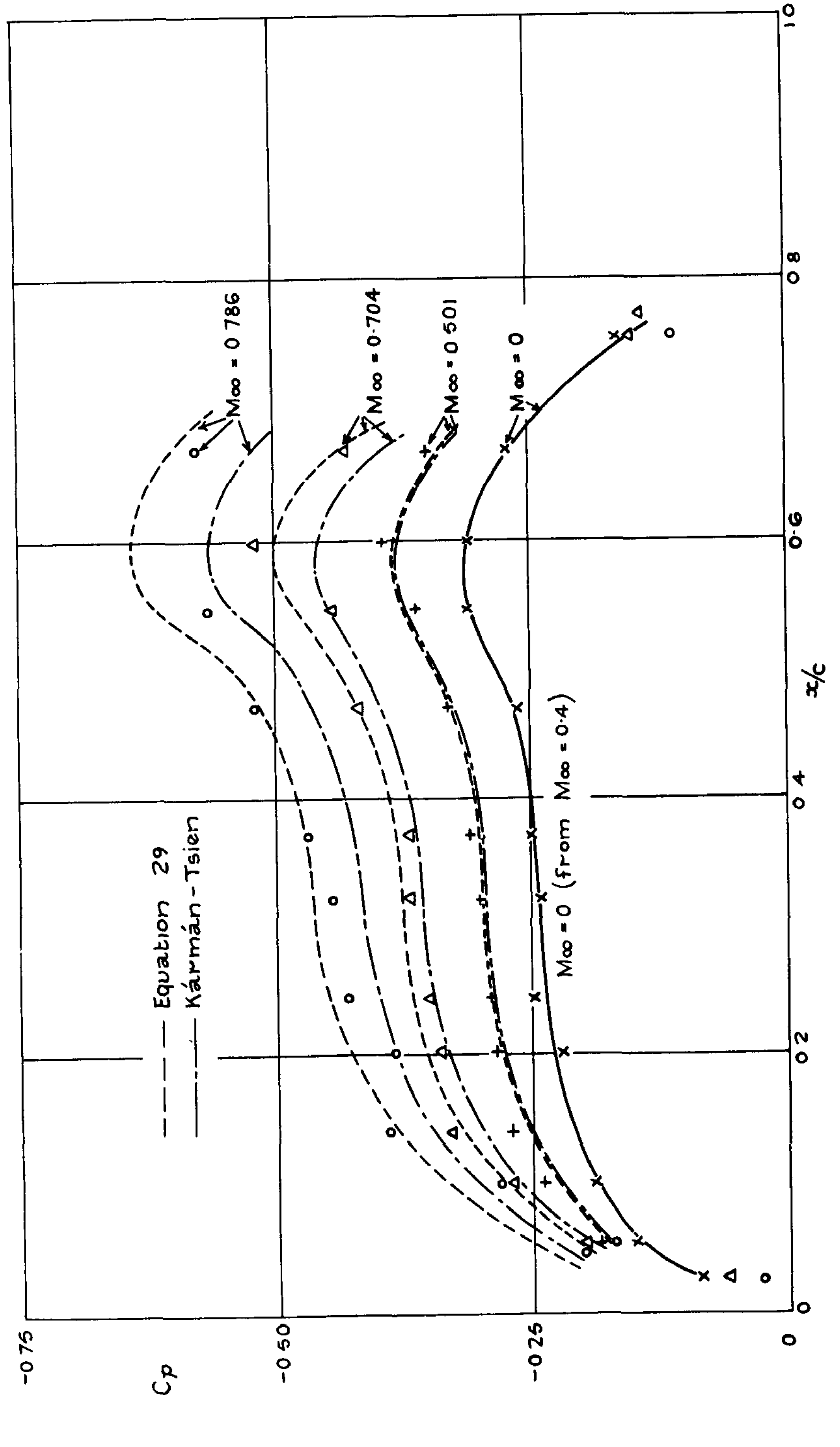

Pressure Distributions on EC 1250 at $\alpha = 0°$

FIG 3

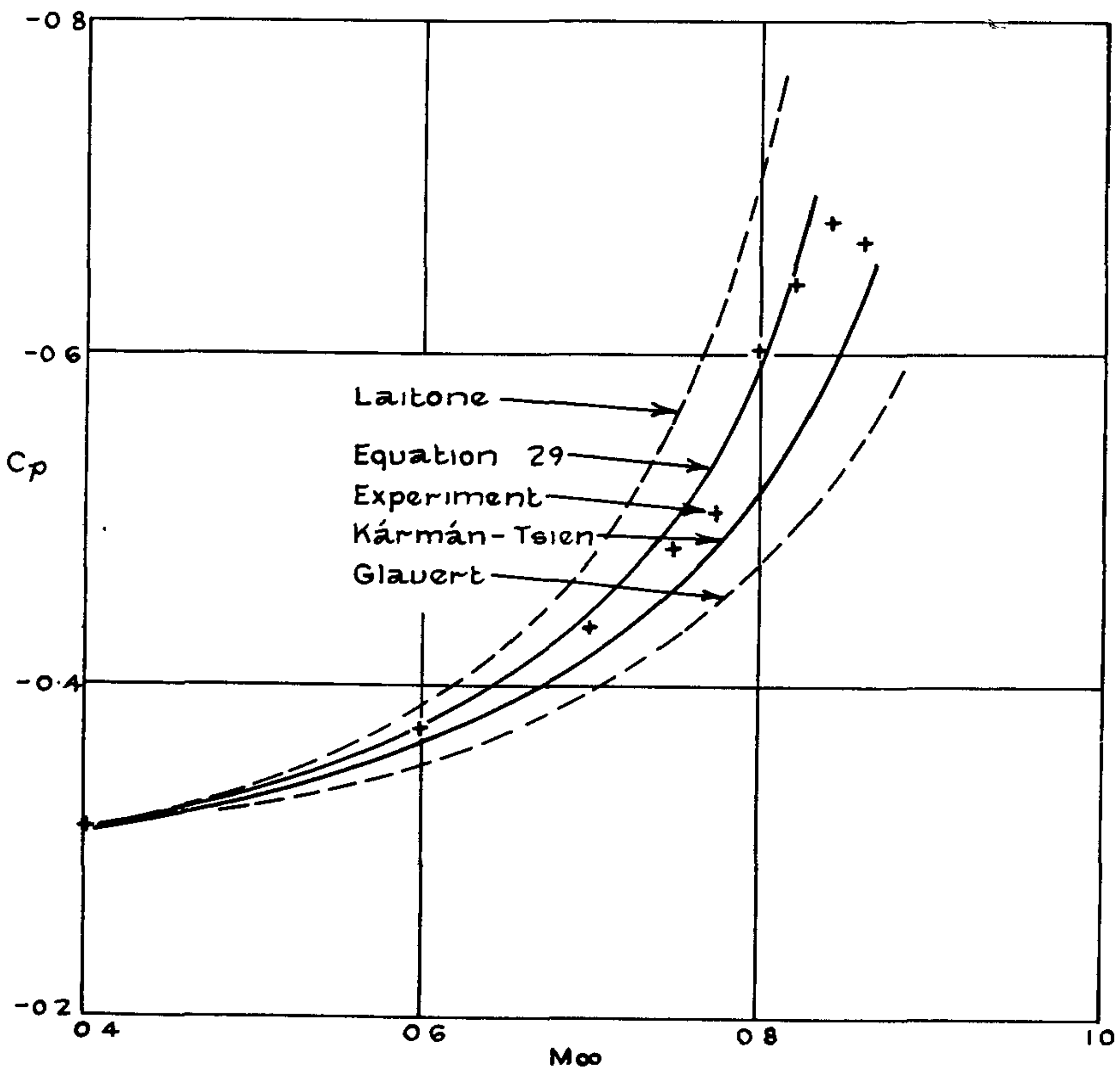

Pressure Coefficients on R.A.E 104 at $x/c = 0{\cdot}44$, $\alpha = 1°$

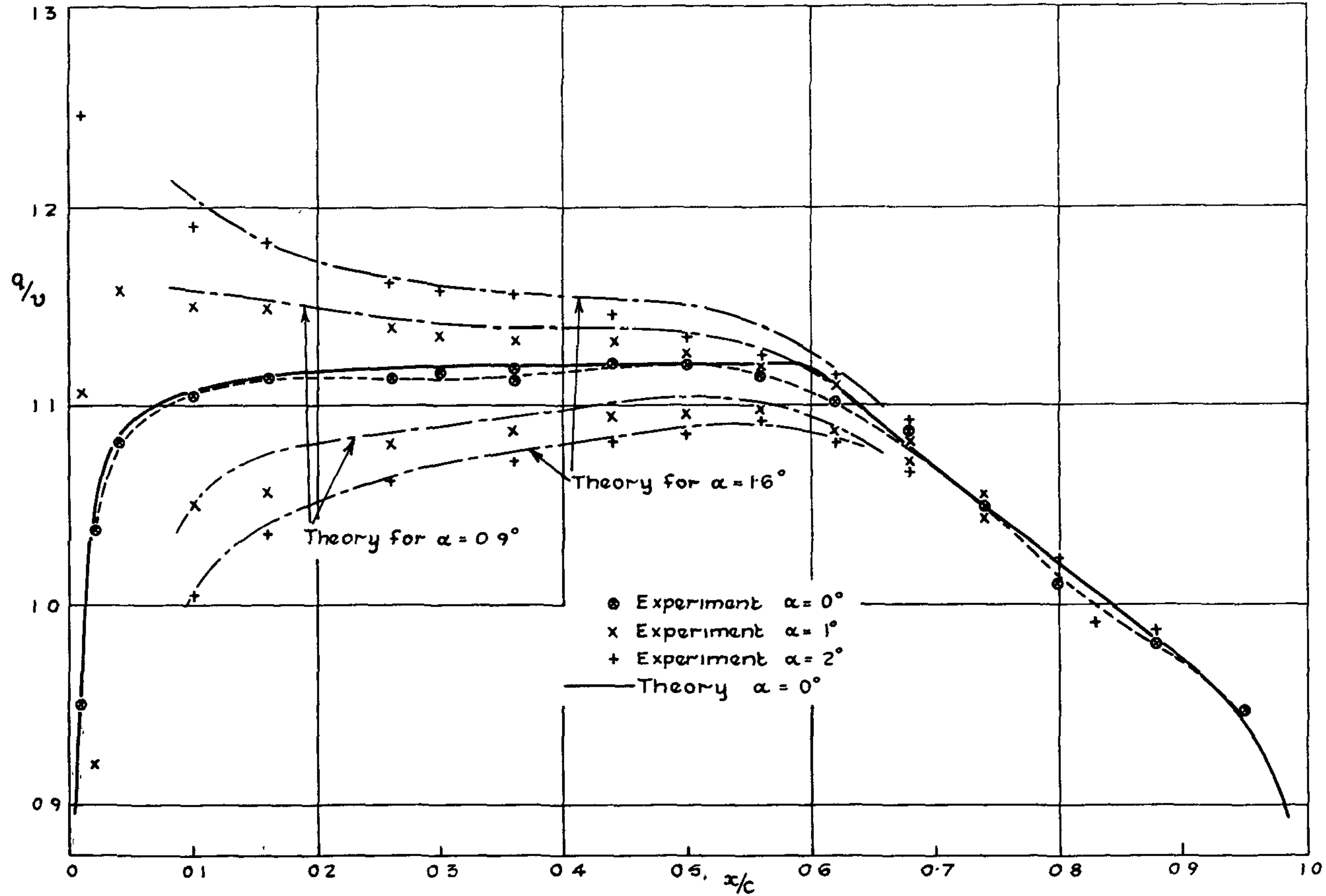

Velocity Distributions for R.A.E. 104 at M∞ = 0

FIG. 4

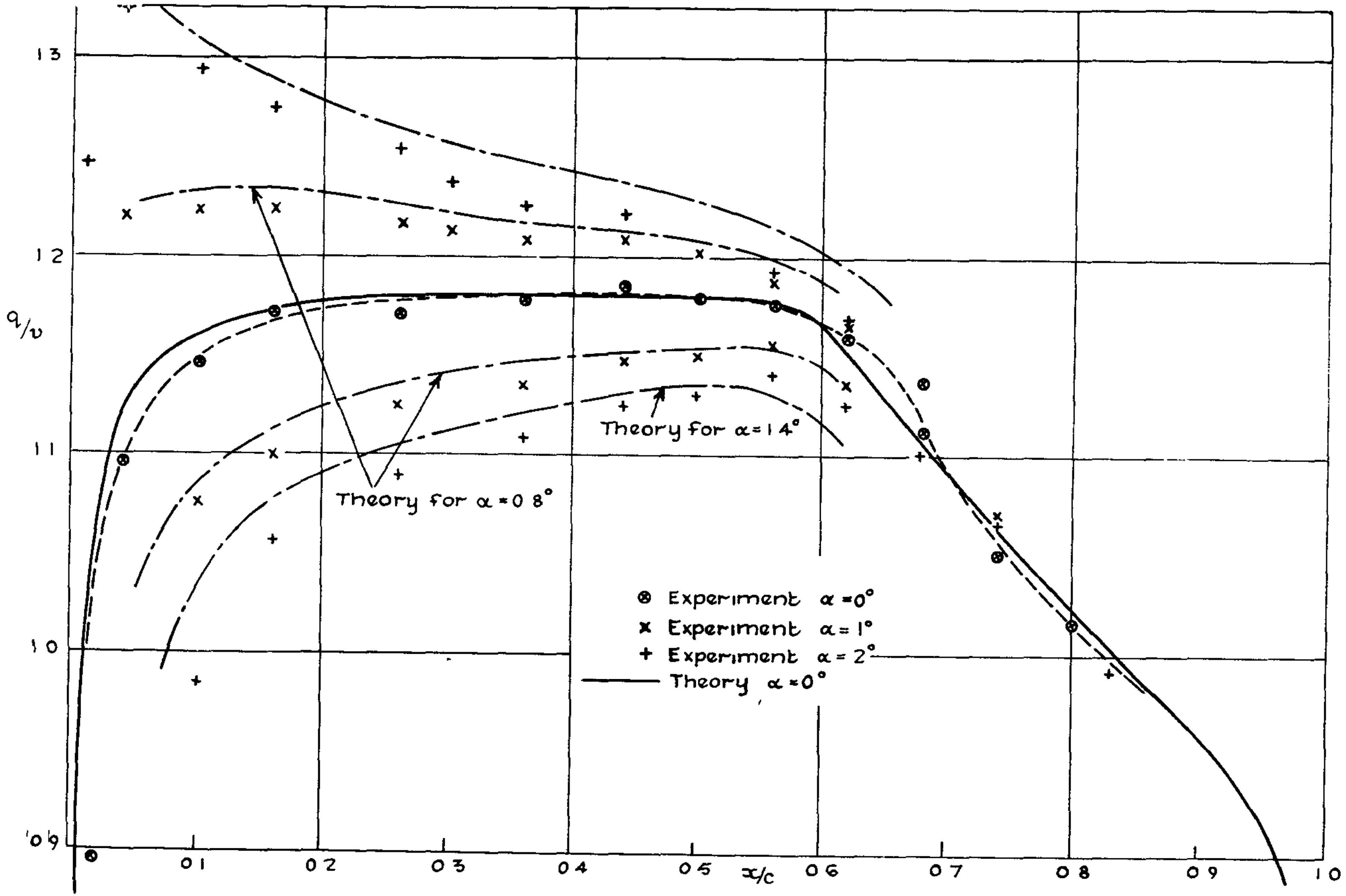

Velocity Distributions for RAE 104 at $M_\infty = 0 \cdot 7$

FIG. 5

32 17

C.P. No. 115
(15,029)
A.R.C. Technical Report

PRINTED AND PUBLISHED BY HER MAJESTY'S STATIONERY OFFICE
To be purchased from
York House, Kingsway, LONDON, W.C.2 423 Oxford Street, LONDON, W.1
P.O. Box 569, LONDON, S.E.1
13a Castle Street, EDINBURGH, 2 1 St. Andrew's Crescent, CARDIFF
39 King Street, MANCHESTER, 2 Tower Lane, BRISTOL, 1
2 Edmund Street, BIRMINGHAM, 3 80 Chichester Street, BELFAST
or from any Bookseller

1953

Price 7s 6d net

PRINTED IN GREAT BRITAIN

S.O. Code No. 23-9007-15